Excited-State Intramolecular Proton Transfer in 2-(3′-Hydroxy-2′-pyridyl)benzoxazole. Evidence of Coupled Proton and Charge Transfer in the Excited State of Some *o*-Hydroxyarylbenzazoles

Sonia Ríos Vázquez, M. Carmen Ríos Rodríguez,* Manuel Mosquera, and Flor Rodríguez-Prieto*

Departamento de Química Física, Facultade de Química, Universidade de Santiago de Compostela, E-15782 Santiago de Compostela, Spain

Received: August 19, 2006; In Final Form: October 18, 2006

The influence of solvent, temperature, and viscosity on the phototautomerization processes of a series of *o*-hydroxyarylbenzazoles was studied by means of ultraviolet−visible (UV−vis) absorption spectroscopy and steady-state and time-resolved fluorescence spectroscopy. The compounds studied were 2-(2′-hydroxyphenyl)-benzimidazole (HBI), 2-(2′-hydroxyphenyl)benzoxazole (HBO), 2-(2′-hydroxyphenyl)benzothiazole (HBT), 2-(3′-hydroxy-2′-pyridyl)benzimidazole (HPyBI), and the new derivative 2-(3′-hydroxy-2′-pyridyl)benzoxazole (HPyBO), this one studied in neutral and acid media. All of these compounds undergo an excited-state intramolecular proton transfer (ESIPT) from the hydroxyl group to the benzazole N3 to yield an excited tautomer in syn conformation. A temperature- and viscosity-dependent radiationless deactivation of the tautomer has been detected for all compounds except HBI and HPyBI. We show that this radiationless decay also takes place for 2-(3-methyl-1,3-benzothiazol-3-ium-2-yl)benzenolate (NMeOBT), the N-methylated analog of the tautomer, whose ground-state structure has anti conformation. In ethanol, the radiationless decay shows intrinsic activation energy for HPyBO and HBO; however, it is barrierless for HBT and NMeOBT and controlled instead by the solvent dynamics. The relative efficiency of the radiationless decay in the series of molecules studied supports the hypothesis that this transition is connected with a charge-transfer process taking place in the tautomer, its efficiency being related to the strength of the electron donor (dissociated phenol or pyridinol moiety) and electron acceptor (protonated benzazole). We propose that the charge transfer is associated with a large-amplitude conformational change of the tautomer, the process leading to a nonfluorescent charge-transfer intermediate. The previous ESIPT step generates the structure with the suitable redox pair to undergo the charge-transfer process; therefore, an excited-state intramolecular coupled proton and charge transfer takes place for these compounds.

Introduction

Proton and electron transfer processes are at the heart of life on Earth. The coupling of proton motion to charge separation is crucial for the most important processes of biological energy conversion: photosynthesis, vision, transmission of the nervous impulses, or respiration. Although a lot of research work has been done on this matter, the detailed molecular mechanism of the coupling of proton and electron transfer remains unclear in many instances.[1−3] In this respect, the design of molecular structures whose photochemical behavior involves coupled proton and electron transfer can provide insight on the subject. On studying the excited-state behavior of various *o*-hydroxyphenylbenzazoles, we found evidence for a process of this type. In this case, an ultrafast excited-state intramolecular proton transfer (ESIPT) induced an intramolecular charge-transfer process.

The excited-state behavior of 2-(2′-hydroxyphenyl)benzimidazole (HBI),[4−12] 2-(2′-hydroxyphenyl)benzoxazole (HBO),[4−7,10,13−31] and 2-(2′-hydroxyphenyl)benzothiazole (HBT)[4−8,13,28−42] (Chart 1) has been a topic of interest for years, HBO being recently proposed as a phototautomerizable model DNA base pair.[20−23] In aprotic solvents, the most stable form of these compounds in the ground state is the intramolecularly hydrogen-bonded normal form $\mathbf{N_{syn}}$ (syn conformation, frequently called cis**)**. In protic solvents, other conformations hydrogen-bonded to the solvent have been detected. Upon excitation of the normal form to its first-excited singlet state, $\mathbf{N^*_{syn}}$, the enhanced acidity of the hydroxyl group causes an ultrafast intramolecular proton transfer from this group to the benzazole nitrogen, affording the planar tautomer $\mathbf{T^*_{syn}}$ (Chart 1). Many research studies have been devoted to studying the dynamics of the ultrafast ESIPT process in the first excited singlet state of HBI, HBO, and HBT, both theoretically and experimentally.[4−6,8,23−28,38−42] The slower dynamics of the proton-transferred tautomer in the picosecond to microsecond time range also has received much attention, including detailed studies of the tautomerization in the triplet state, for which only scarce studies exist for other ESIPT molecules.[4−7,9−18,29−38]

Despite the general similarities observed for the *o*-hydroxyphenylbenzazoles, markedly different fluorescence quantum yields and lifetimes were measured for these compounds, much higher values being observed for HBI than for HBO and HBT.[5] Moreover, the fluorescence quantum yield and lifetime of HBI showed no significant temperature dependence (except for the effect of the varying amounts of ground-state conformers

* Authors to whom correspondence should be addressed. E-mail addresses: for M.C.R.R., qfcaryrr@usc.es; for F.R.-P., qfflorrp@usc.es.

10.1021/jp0653813 CCC: $37.00
Published on Web 02/20/2007

CHART 1: Molecular Structures of HBI, HBO, HBT, HPyBI, and HPyBO, Their Tautomers (N_{syn}, T_{syn} and T_{anti}), the Methylated Derivatives OMePyBO and NMeOBT, and the Quaternary Salts NMeBI, NMeBO, and NMeBT

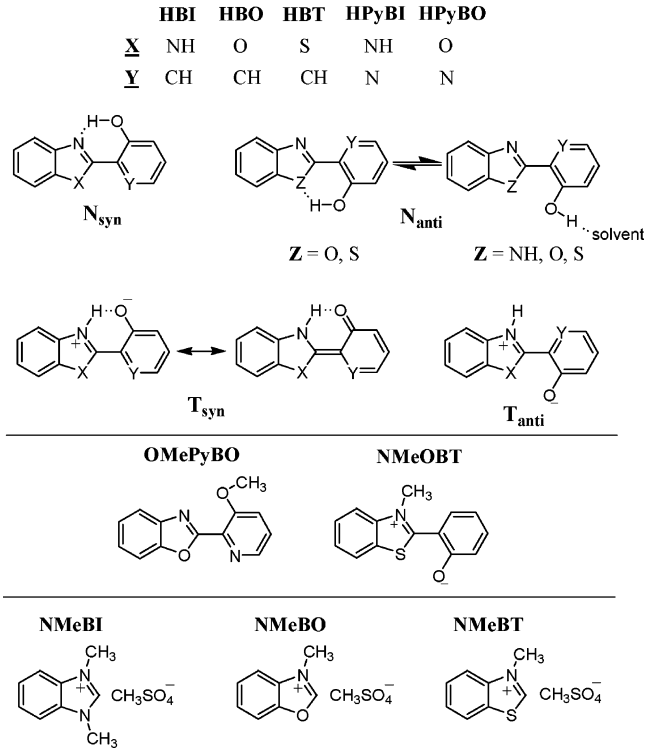

hydrogen-bonded to alcoholic solvents),[10] whereas for HBO and HBT, they decreased as the temperature rose, reaching very low values at room temperature.[5] Various authors showed that this fact is due to a temperature-dependent radiationless deactivation of the proton-transferred form $\mathbf{T^*_{syn}}$; however, the nature of this deactivation process remains unclear.[4−6,14,33,34,37,38] It has been proved that the thermally activated decay does not involve intersystem crossing, but it is associated with a syn−anti isomerization.[15,16,32,33] The anti rotamer $\mathbf{T_{anti}}$ (Chart 1; this conformation is often called trans**)** has been experimentally detected by transient absorption measurements and two-step laser excitation as a long-lived transient ground-state species for HBT and HBO.[16,30−34] Detailed temperature-dependent studies carried out by Al-Soufi et al.[33] on the mechanism of isomerization for HBT concluded that at least two different thermally activated deactivation channels must exist for $\mathbf{T^*_{syn}}$. They proposed two alternative mechanisms that could account for their observations: one of them includes a twisted species as an intermediate, which, in the ground state, would relax to $\mathbf{T_{syn}}$ or $\mathbf{T_{anti}}$, and the other includes the formation of the anti tautomer in the excited state and an additional activated internal conversion of $\mathbf{T^*_{syn}}$.

The radiationless decay of the $\mathbf{T^*_{syn}}$ form of HBT becomes slower as the solvent viscosity increases,[32,37,38] which was explained by the contribution of high-amplitude motions to the radiationless decay (twisting about the interannular bond has been suggested). Moreover, Potter et al. proposed that an intramolecular charge transfer (CT) process in $\mathbf{T^*_{syn}}$ might induce the interannular bond rotation, leading to a non-emissive, twisted excited state.[37] A similar process has been presented for related structures.[43−45]

ESIPT and a very fast radiationless decay are the key features in the mechanism of action of many UV photostabilizers, such as 2-(2′-hydroxy-5′-methylphenyl)benzotriazole, 2-(2′-hydroxyphenyl)-1,3,5-triazine, and derivatives.[46] They show a similar photophysical behavior to HBO and HBT (ultrafast ESIPT and a very effective temperature- and viscosity-dependent radiationless decay of the proton-transferred form); however, they are much better photostabilizers, presumably because the radiationless decay of the tautomer is more efficient. Therefore, it is very important for the design of new photostabilizers to know the factors that contribute to a fast radiationless deactivation, and many research studies were devoted to unravel the photophysics of this family of compounds by theoretical and experimental methods.[47−55] On the other hand, HBO and HBT were explored for nonlinear optical applications and light-emitting devices.[56−58] These and other ESIPT dyes were also examined for a wide range of applications, including the above-mentioned UV photostabilizers, fluorescence sensors, laser dyes, data storage, optical switches, UV filters, etc.[41,59] On that account, a better knowledge of the photophysical properties of ESIPT dyes may contribute to the improvement of their technological applications.

To provide insight into the mechanism of the thermally activated radiationless decay of *o*-hydroxyarylbenzazoles, we decided to investigate the relationship between the effectiveness of the radiationless deactivation and the electron donor and acceptor strength of different model compounds. The series of *o*-hydroxyarylbenzazoles (Chart 1) was formed by HBO, HBT, (3-methyl-1,3-benzothiazol-3-ium-2-yl)benzenolate (NMeOBT), the new compound 2-(3′-hydroxy-2′-pyridil)benzoxazole (HPyBO), and the benzimidazole analogs HBI and HPyBI, previously studied by our group.[12,60]

In this article, we report the first studies of the ground- and excited-state behavior of the new ESIPT molecule HPyBO in neutral and acidified solvents, and we investigate the fluorescence of the series of *o*-hydroxyarylbenzazoles described above, both at room temperature in solvents of various viscosities and as a function of temperature (mainly in ethanol and 2-butanol). The main objectives of this study are (1) to investigate the photophysics of HPyBO in neutral and acid media, (2) to get information about the temperature and viscosity dependence of the radiationless deactivation process experienced by different *o*-hydroxyarylbenzazoles, and (3) to test the hypothesis that an intramolecular charge transfer induces the radiationless deactivation of these compounds.

Experimental Section

Materials. HBO and HBT were provided by Kodak and Aldrich, respectively. HBI and HPyBI were synthesized as described elsewhere.[12,60]

HPyBO was prepared by high-temperature condensation of 14 mmol of 3-hydroxy-2-pyridinecarboxylic acid (Aldrich) with 20 mmol of 2-aminophenol (Aldrich) at ∼150 °C, and the product was purified by column chromatography. ^{1}H NMR (300 MHz, dimethyl sulfoxide-d_6), δ (ppm): 7.51 (m, 4H), 7.87 (m, 2H), 8.31 (m, 1H), 11.22 (s, 1H). MS, *m*/*z* (relative intensity): 212 (100, M^+), 118 (40).

A stock solution of OMePyBO was obtained by slowly adding 0.06 mmol of CH_3I dropwise over a solution of 0.03 mmol of HPyBO in dimethyl sulfoxide (5 mL) previously basified with 0.1 mmol of KOH. After stirring the mixture at room temperature for 2 h, the excess of KOH was filtrated.

NMeOBT was prepared by heating a mixture of 9 mmol of HBT (Kodak) with 55 mmol of dimethyl sulfate at 100 °C for 48 h. The hot reaction mixture was then slowly poured over a large amount of acetone. The solid obtained was dissolved in

ethanol and filtrated to separate the insoluble impurities. The solvent was then evaporated and the solid recrystallized from acetone. ^{1}H NMR (300 MHz, $CDCl_3$), δ (ppm): 4.05 (s, 3H), 7.07 (d, 1H, $J = 8.0$ Hz), 7.14 (t, 1H, $J = 8.0$ Hz), 7.38 (t, 1H, t, $J = 8.0$ Hz), 7.48 (m, 2H), 7.93 (d, 1H, $J = 8.1$ Hz), 8.11 (d, 1H, $J = 7.9$ Hz), 8.54 (dd, 1H, $J = 8.0$ Hz, $J = 1.9$ Hz).

3-Methylbenzimidazolium methyl sulfate (NMeBI; Chart 1) was synthesized by stirring, at room temperature, 15 mmol of benzimidazole (Fluka) in the presence of 15 mL of dimethyl sulfate for 1 h. The product was then filtrated and washed with acetone, to remove the excess dimethyl sulfate. ^{1}H NMR (300 MHz, dimethyl sulfoxide-d_6), δ (ppm): 3.37 (s, 3H), 4.08 (s, 6H), 7.70 (dd, 2H, $J = 6.2$ Hz, $J = 3.1$ Hz), 8.02 (dd, 2H, $J = 6.2$ Hz, $J = 3.1$ Hz), 9.63 (s, 1H). MS, *m*/*z* (relative intensity): 147 (100, M − (CH_3SO_4)), 405 (36, M + 147)).

3-Methylbenzoxazolium methyl sulfate (NMeBO; Chart 1) was obtained by adding 20 mmol of melted benzoxazole (Aldrich) to 20 mmol of dimethyl sulfate and stirring the mixture for 2 h. The solid obtained was washed with ether and acetone. The crystals obtained (hygroscopic) were stored in ether. ^{1}H NMR (300 MHz, dimethyl sulfoxide-d_6), δ (ppm): 3.36 (s, 3H), 4.20 (s, 3H), 7.83 (m, 2H), 8.2 (m, 2H), 10.60 (s, 1H). MS, *m*/*z* (relative intensity): 134 (100, M − (CH_3SO_4)), 379 (12, M + 134).

3-Methylbenzothiazolium methyl sulfate (NMeBT; Chart 1) was prepared by stirring, at room temperature, 46 mmol of benzothiazole (Fluka) with 105 mmol of dimethyl sulfate for 30 min. The solution was then neutralized with triethylamine, and the product was precipitated from the reaction mixture by adding acetone. The crystals obtained were washed with acetone. ^{1}H NMR (300 MHz, dimethyl sulfoxide-d_6), δ (ppm): 3.37 (s, 3H), 4.40 (s, 3H), 7.85 (t, 1H, $J = 8.0$ Hz), 7.94 (t, 1H, $J = 8.0$ Hz), 8.32 (d, 1H, $J = 8.0$ Hz), 8.50 (d, 1H, $J = 8.0$ Hz), 10.53 (s, 1H). MS, *m*/*z* (relative intensity): 150 (100, M − (CH_3SO_4)), 411 (31, M + 150).

Methods. Solutions were made up in double-distilled water and spectroscopy-grade solvents and were not degassed. The acidity, in aqueous solutions, was varied with a NaH_2PO_4/Na_2HPO_4 buffer (made up with Merck p.a. products). The acidified nonaqueous solutions of HPyBO and OMePyBO were prepared adding $HClO_4$ to the solution until the UV−vis absorption spectrum of the monocation was obtained. Concentrations of $\sim 10^{-5}$ mol dm^{-3} for absorption and $\sim 10^{-6}$ mol dm^{-3} for fluorescence were employed. All experiments were carried out at 25 °C, except otherwise stated.

The pH was measured with a Radiometer model PHM 82 pH meter equipped with a Radiometer Type B combined electrode. UV−vis absorption spectra were recorded in a Varian Cary 3E spectrophotometer. Fluorescence excitation and emission spectra were recorded in a Spex model Fluorolog-2 FL340 E1 T1 spectrofluorometer, with correction for instrumental factors by means of a Rhodamine B quantum counter and correction files supplied by the manufacturer. UV−vis absorption and fluorescence measurements at low temperature were performed using an Oxford Instruments liquid nitrogen cryostat (model 1704) with a model ITC503 control unit, and the spectra obtained were corrected for the temperature dependence of the solution volume. Fluorescence quantum yields were measured using quinine sulfate ($< 3 \times 10^{-5}$ mol dm^{-3}) in aqueous H_2SO_4 (0.5 mol dm^{-3}) as a standard ($\phi = 0.546$).[61,62] Fluorescence lifetimes were determined by time-correlated single-photon counting in an Edinburgh Instruments model FL-900 spectrometer equipped with a hydrogen-filled nanosecond flashlamp and the reconvolution analysis software supplied by the manufacturer.

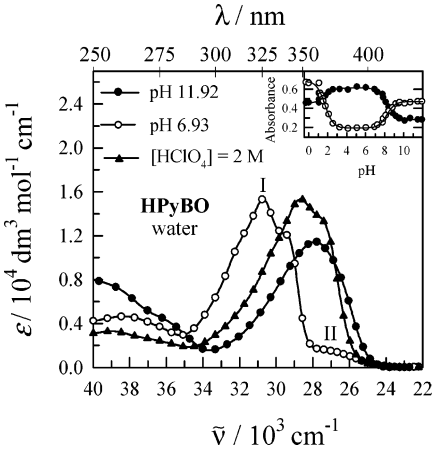

Figure 1. Absorption spectra of HPyBO in neutral, acidic, and basic aqueous solutions; the inset shows the pH dependence of the absorbance of HPyBO in aqueous solution at (○) 28 570 cm^{-1} and (●) 30 300 cm^{-1}.

Cyclic voltammetry measurements were performed using an Autolab potentiostat galvanostat model PGSTAT 20 and a saturated Ag/AgCl reference electrode in acetonitrile solution. Theoretical equations were fitted to experimental data by means of a nonlinear weighted least-squares routine based on the Marquardt algorithm.

Results

1. Absorption Spectra, Fluorescence Spectra, and Lifetimes of HPyBO. The absorption spectra of HPyBO in aqueous solution under acidic, neutral, and basic conditions are shown in Figure 1. The absorption spectrum in neutral media showed an intense band (band I) peaking at 30 700 cm^{-1}, accompanied by a weak band (band II) located at ~27 000 cm^{-1}. Increasing or decreasing the pH shifted the absorption spectrum to the red, and new bands, with maxima at 27 900 cm^{-1} (pH 12) and 28 700 cm^{-1} ([$HClO_4$] = 2 mol dm^{-3}), were detected. The inset of Figure 1 shows the pH dependence of the absorbance at 30 300 cm^{-1} and 28 570 cm^{-1}.

The fluorescence spectra of OMePyBO in methanol are shown in Figure 2a. The excitation and emission spectra were independent of the monitoring wavenumber and overlapped. The fluorescence decay was monoexponential, with a decay time (see Table 1) of 1.3 ns. In acidified methanol, both the excitation and the emission spectra showed only one band, overlapped, and were red-shifted with respect to those measured in neutral methanol.

Both the excitation and the emission spectra of HPyBO in acetonitrile depended on the monitoring wavenumber (Figure 2b). The emission spectra exhibited dual fluorescence, with a strong lower-energy (red) band and a very weak higher-energy (blue) band. The position of the blue band was very similar to that of the emission spectrum of the methoxy derivative in methanol (Figure 2a). The excitation spectrum recorded at the higher-energy emission band was blue-shifted with respect to the absorption band and similar to the excitation spectrum obtained for OMePyBO in methanol. However, the excitation spectrum monitored at the red-emission band almost matched the absorption spectrum measured in the same solvent; this means that the species yielding the red-emission band upon excitation is virtually the only absorbing species. Under this assumption, the fluorescence quantum yield of the red-emission

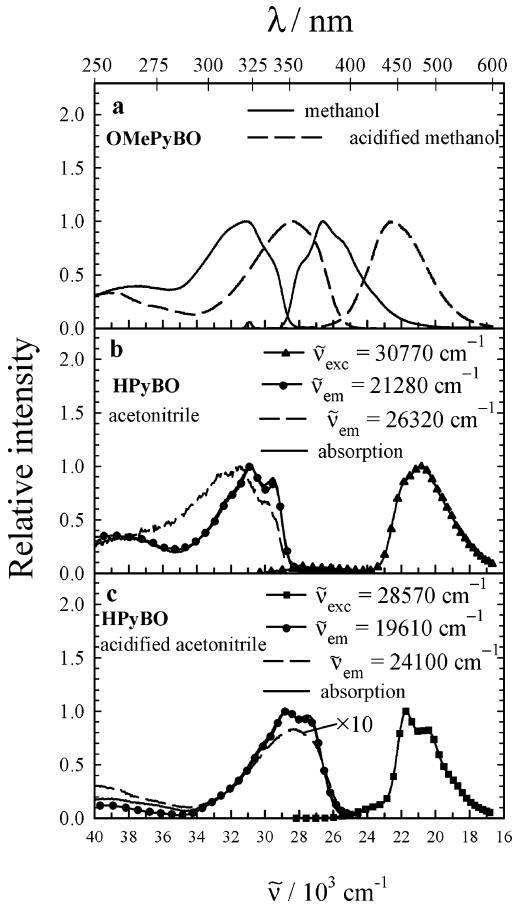

Figure 2. Normalized fluorescence excitation and emission spectra of (a) OMePyBO in neutral ($\tilde{\nu}_{em}$ = 26 670 cm^{-1}, $\tilde{\nu}_{exc}$ = 31 250 cm^{-1}) and acidified methanol ($\tilde{\nu}_{em}$ = 22 730 cm^{-1}, $\tilde{\nu}_{exc}$ = 28 570 cm^{-1}); (b) HPyBO in acetonitrile, together with the absorption spectrum in the same solvent; and (c) HPyBO in acidified acetonitrile, together with the absorption spectrum in the same solvent.

band was calculated to be 0.013. A similar procedure in other solvents (spectra not shown here) led to the fluorescence quantum yields ϕ_T listed in Table 2. Furthermore, the fluorescence decay of HPyBO in acetonitrile was monoexponential (Table 1), both at the blue-emission band (decay time τ_N = 1.27 ns) and at the maximum of the red-emission band (decay time τ_T = 0.25 ns).

The fluorescence spectra of HPyBO were also recorded in acetonitrile acidified with $HClO_4$ until all the neutral form was protonated. The emission spectrum (Figure 2c) showed an intense band at 21 740 cm^{-1}, accompanied by a weak shoulder (∼24 000 cm^{-1}) located at about the same position as the emission spectrum of the methoxy derivative in acidified methanol. The excitation spectrum obtained at $\tilde{\nu}_{em}$ = 24 100 cm^{-1} was very similar to that detected for OMePyBO in acidified methanol. Moreover, the excitation spectrum monitored at the emission maximum almost coincided with the absorption spectrum registered for HPyBO in acidified acetonitrile. The fluorescence decay measured at $\tilde{\nu}_{em}$ < 22 000 cm^{-1} was monoexponential with a decay time of 2.6 ns (Table 1). The global fluorescence quantum yields (measured under excitation at the maximum of the absorption band) obtained in various solvents are compiled in Table 2.

The fluorescence spectra of HPyBO in ethanol within the temperature range of 165−295 K are shown in Figure 3, together with those recorded in neutral and acidified acetone at temperatures between 180 K and ∼295 K. In ethanol, upon increasing the temperature (Figure 3a), the intensity of the two emission bands markedly decreased. In acetone, only the red-emission band was present, its intensity drastically decreasing as the temperature increased (Figures 3b and 4b). In acidified acetone, however, only a slight decrease of intensity was observed when the temperature was increased (Figure 3c).

The fluorescence decays of HPyBO and HPyBI in ethanol, measured at the maximum of the red-emission band between 165 K and room temperature, were monoexponential and led to the decay times shown in Figure 4a. Whereas for HPyBI, the decay time was virtually independent of temperature (∼4.1 ns), for HPyBO, a marked reduction (from 4.2 ns at 165 K to 0.82 ns at 292 K) was observed when the temperature was increased.

2. Influence of Solvent and Temperature on the Fluorescence of HBI, HBO, HBT, and NMeOBT. Figure 5 shows the fluorescence spectra of HBO and HBT in ethanol and 2-butanol in the temperature range of 165−300 K. For HBO (Figures 5a and 5b), the fluorescence spectra at 165 K showed an intense band at ∼20 500 cm^{-1}, whose intensity drastically decreased when the temperature was increased, together with a very weak band at ∼26 000 cm^{-1}, with its intensity decreasing as the temperature increased. A similar behavior was observed for HBT (Figures 5c and 5d), except for the fact that the intensity of the red-emission band was much weaker than that of HBO.

Dual fluorescence was also observed in other solvents for both HBO and HBT (spectra not shown). In all cases, the species leading to the red-emission band was the only significant absorbing species at room temperature, as the excitation spectrum monitored at this band matched the absorption spectrum. Therefore, the fluorescence quantum yield of the red-emission band (ϕ_T) of HBO and HBT could be obtained at room temperature in solvents of various viscosities. The data obtained are given in Table 2, together with the values measured for HBI. It is observed that, for the same solvent, ϕ_T(HBI) ≫ ϕ_T(HBO) > ϕ_T(HBT). Furthermore, for HBO and HBT, the fluorescence quantum yield increased with the viscosity of the solvent, whereas, for HBI, it showed no viscosity dependence.

The excitation and emission spectra of NMeOBT in various alcohols are given in Figure 6a. The emission spectrum in glycerol, located at ∼18 000 cm^{-1}, overlapped the excitation spectrum and both spectra were independent of the monitoring wavenumber. The behavior in ethylene glycol and methanol was very similar, except for a slight shift of the emission spectra to the red upon going from glycerol to methanol. The fluorescence quantum yields (ϕ_T) measured in various alcohols are listed in Table 2. The values obtained were even lower than those measured for HBO and HBT and increased with the solvent viscosity. The fluorescence of NMeOBT was also recorded in ethanol and 2-butanol (Figures 6b and 6c) at various temperatures between 165 K and room temperature, a strong decrease in intensity being observed as the temperature increased. The fluorescence quantum yield was measured in both solvents as a function of temperature (Figure 7c), a higher ϕ_T being observed in the more-viscous 2-butanol than in ethanol at any temperature.

Time-resolved fluorescence was measured as a function of temperature for HBO in ethanol and 2-butanol, and for HBI and HBT in ethanol. The fluorescence decay was monoexponential at any emission wavenumber for HBI and at the red-emission band for HBO and HBT, yielding the decay times shown in Figures 7a and 7b. Whereas the decay time observed for HBI (∼4.7 ns) was independent of temperature over the whole temperature range studied (170−285 K), those of HBO and HBT decreased as the temperature increased. The fluores-

TABLE 1: Fitted Values of the Fluorescence Decay Times (τ) of HPyBO in Neutral and Acidified Acetonitrile and of OMePyBO in Methanol at 298 K

compound	solvent	$\tilde{\nu}_{exc}$/cm^{-1}	$\tilde{\nu}_{em}$/cm^{-1}	τ_N/ns	τ_T/ns	τ_{TC}/ns	χ^2
HPyBO	acetonitrile	30770	25970	1.271 ± 0.005			0.935
HPyBO	acetonitrile	30770	20000		0.247 ± 0.004		1.148
HPyBO	acidified acetonitrile	27780	21980			2.654 ± 0.003	1.098
HPyBO	acidified acetonitrile	27780	20000			2.573 ± 0.003	1.033
HPyBO	acidified acetonitrile	27780	18870			2.571 ± 0.003	1.079
OMePyBO	methanol	30770	26670	1.275 ± 0.002			1.125
OMePyBO	methanol	30770	25000	1.296 ± 0.002			1.107

TABLE 2: Fluorescence Quantum Yields of the Species Studied in this Work at 298 K in Solvents of Various Viscosities

		HPyBO		ϕ_T[a]				
solvent	$\eta_{293.15\,K}$/cP[b]	ϕ_{acid}[c]	ϕ_T[d]	HPyBI[e]	HBI	HBO	HBT	NMeOBT
diethyl ether	0.24	0.08	0.010			0.0032	0.0005	
n-hexane	0.31			0.44				
acetonitrile	0.36	0.14	0.013	0.49	0.25	0.0026	0.0003	
tetrahydrofuran	0.55		0.012		0.22	0.0032	0.0005	
methanol	0.55	0.10	0.024	0.52[f]	0.15	0.0026	0.0006	0.0003
2-butanol	4.21				0.20	0.0062	0.0019	0.0009
ethylene glycol	19.9	0.07	0.065		0.16	0.0120	0.0036	0.0015
glycerol	1412	0.08	0.101			0.0332	0.0222	0.0113

[a] Here, ϕ_T represents the fluorescence quantum yield of NMeOBT and that of the red-shifted fluorescence of HPyBI, HBI, HBO, and HBT. [b] From ref 77. [c] ϕ_{acid} represents the fluorescence quantum yield in acidified solvents. [d] Here, ϕ_T represents the fluorescence quantum yield of the red-shifted fluorescence of HPyBO. [e] From ref 60. [f] Value in ethanol.

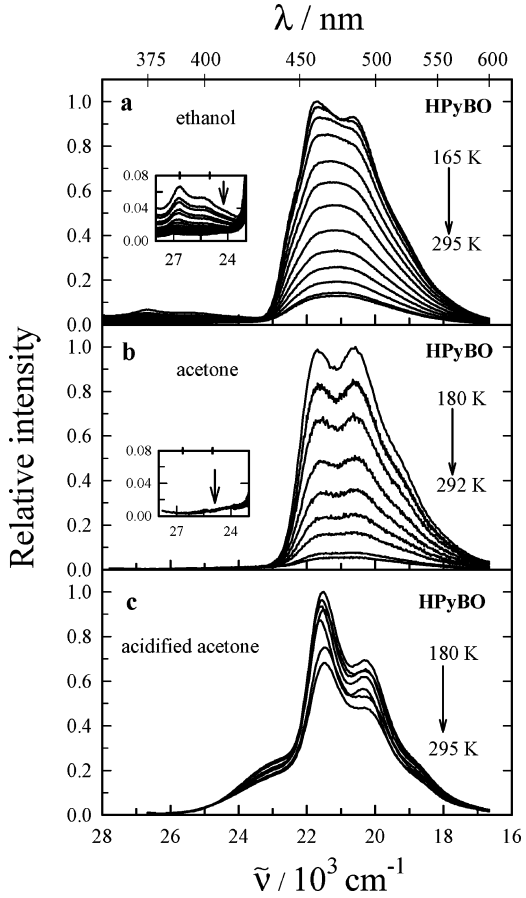

Figure 3. Fluorescence spectra of HPyBO (a) in ethanol in the temperature range of 165−295 K, with $\tilde{\nu}_{exc}$ = 30 770 cm^{-1}; (b) in acetone in the temperature range of 180−292 K, with $\tilde{\nu}_{exc}$ = 30 770 cm^{-1}; and (c) in acidified acetone in the temperature range of 180−295 K, with $\tilde{\nu}_{exc}$ = 27 400 cm^{-1}.

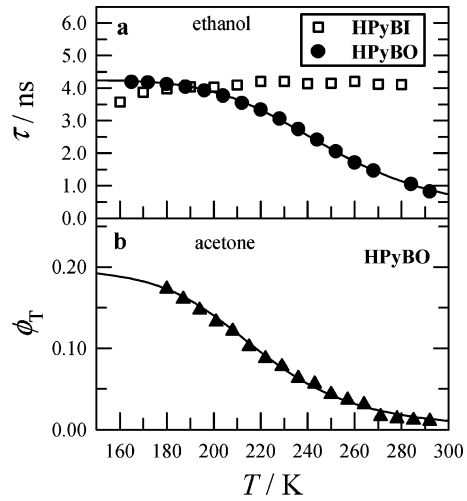

Figure 4. Temperature dependence of (a) the fluorescence decay times τ_T of HPyBO (obtained from the monoexponential fit of the fluorescence decay at $\tilde{\nu}_{exc}$ = 29 850 cm^{-1} and $\tilde{\nu}_{em}$ = 21 050 cm^{-1}) and of HPyBI (obtained from the monoexponential fit of the fluorescence decay at $\tilde{\nu}_{exc}$ = 30 300 cm^{-1} and $\tilde{\nu}_{em}$ = 22 700 cm^{-1}) in ethanol, together with the fit of eq 1 to the data of HPyBO; and (b) the fluorescence quantum yield ϕ_T of HPyBO in acetone (calculated from the spectra of Figure 3b), together with the fit of eq 2 to the experimental data.

cence lifetime of HBO at low temperature had a value similar to that of HBI at any temperature.

3. Redox Properties of Benzazoles. Cyclic voltammetry measurements were performed in acetonitrile for the quaternary benzazolium salts NMeBI, NMeBO, and NMeBT (see Chart 1). Experiments were carried out at various scan rates and sample concentrations, and, in all cases, quasi- or totally irreversible waves were obtained. Consequently, the reduction potentials of all these compounds could not be obtained. However, a qualitative analysis of the relative oxidizing strength of the quaternary salts can be done by comparing the reduction peak potentials E_p of the voltammograms of these compounds if the experiments are performed at the same sample concentration and scan rate. The waves measured at a sample concentration of 0.02 mol dm^{-3} and 100 mV/s for these salts led to reduction peak potentials of −2.1, −1.6, and −1.4 V for NMeBI, NMeBO, and NMeBT, respectively.

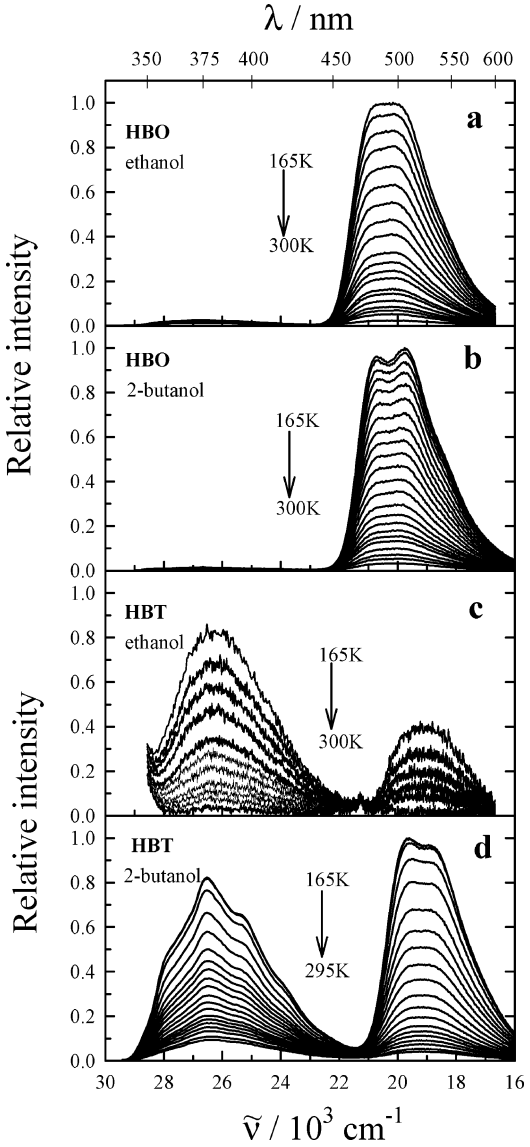

Figure 5. Fluorescence spectra of (a) HBO in ethanol in the temperature range of 165−300 K, with $\tilde{\nu}_{exc} = 31\,250$ cm^{-1}; (b) HBO in 2-butanol in the temperature range of 165−300 K, with $\tilde{\nu}_{exc} = 30\,300$ cm^{-1}; (c) HBT in ethanol in the temperature range of 165−300 K, with $\tilde{\nu}_{exc} = 29\,410$ cm^{-1}; and (d) HBT in 2-butanol in the temperature range of 165−295 K, with $\tilde{\nu}_{exc} = 30\,300$ cm^{-1}.

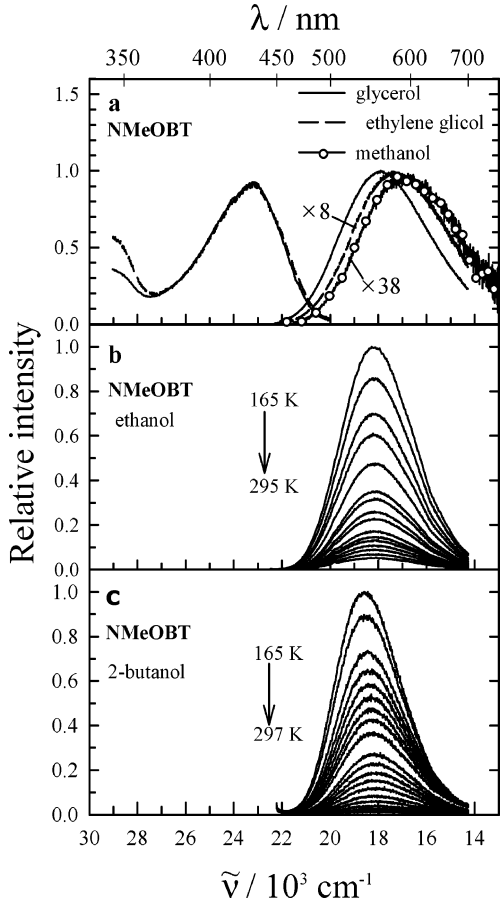

Figure 6. (a) Normalized fluorescence excitation and emission spectra of NMeOBT in glycerol ($\tilde{\nu}_{em} = 17\,860$ cm^{-1}, $\tilde{\nu}_{exc} = 23\,260$ cm^{-1}) and ethylene glycol ($\tilde{\nu}_{em} = 17\,000$ cm^{-1}, $\tilde{\nu}_{exc} = 23\,500$ cm^{-1}), together with the emission spectrum in methanol ($\tilde{\nu}_{exc} = 22730$ cm^{-1}). (b) Fluorescence spectra of NMeOBT in ethanol in the temperature range of 165−295 K, with $\tilde{\nu}_{exc} = 22\,730$ cm^{-1}. (c) Fluorescence spectra of NMeOBT in 2-butanol in the temperature range of 165−297 K, with $\tilde{\nu}_{exc} = 22\,730$ cm^{-1}.

Discussion

1. Interpretation of the Absorption Spectra of HPyBO in Aqueous Solution: Tautomeric and Acid−Base Equilibria in the Ground State. A global analysis of the absorbance−pH data of HPyBO at various fixed wavenumbers in the pH range of 0−12 led to the values p$K_{a1} = 1.67 \pm 0.06$ and p$K_{a2} = 8.24 \pm 0.05$ for the protonation and deprotonation equilibria observed (Figure 1).

The only acidic site of HPyBO is the hydroxyl group, and, thus, the absorption spectrum at basic pH must correspond to the anion deprotonated at the OH group. This spectrum is similar to that of the anion of the benzimidazole derivative HPyBI,[60] also deprotonated at the hydroxyl group, and the pK_a value is also close to that obtained by us for HPyBI (8.57).[63]

The absorption spectrum of HPyBO in neutral aqueous solution, which must correspond to the neutral species, showed two lower-energy bands, labeled bands I and II in Figure 1. Two similar absorption bands were also reported by us for the benzimidazole analogs HPyBI[60] and HBI,[12] and for 4,5-dimethyl-2-(2′-hydroxyphenyl)imidazole,[64] and respectively assigned to the "normal" form, possessing an OH group, and its tautomer generated by proton transfer from the hydroxyl group to the benzimidazole N3. A similar ground-state equilibrium must take place for HPyBO in aqueous solution, absorption bands I and II respectively corresponding to the neutral form **N** and its tautomer **T** (Chart 1). **T** can have a syn or anti conformation and can be written in two limiting resonant structures: zwitterionic or ketonic (Chart 1). According to a theoretical study on 4,5-dimethyl-2-(2′-hydroxyphenyl)imidazole, **T** has a greater zwitterionic character in polar solution.[65] Becker et al. also proposed a zwitterionic structure for the HBT tautomer, based on the solvatochromic shift of its absorption spectrum.[34]

The absorbance relation A_{II}/A_I, and so probably the concentration relation [**T**]/[**N**], is lower for HPyBO (∼0.1) than for HPyBI (∼0.4)[60] and for 4,5-dimethyl-2-(2′-hydroxyphenyl)imidazole (∼0.8)[64] but is slightly greater than that for HBI (∼0.06).[12] Band II does not appear in the absorption spectrum in acetonitrile (Figure 2b), which means that the equilibrium amount of **T** is much lower in this solvent. Similar behavior was found for HBI,[12] HPyBI,[60] and 4,5-dimethyl-2-(2′-hydroxyphenyl)imidazole,[64] for which the ground-state tautomer was detected only in aqueous solution. According to theoretical studies, this fact is mainly due to the differential stabilization of the highly polar tautomer structure by solute−solvent electrostatic interac-

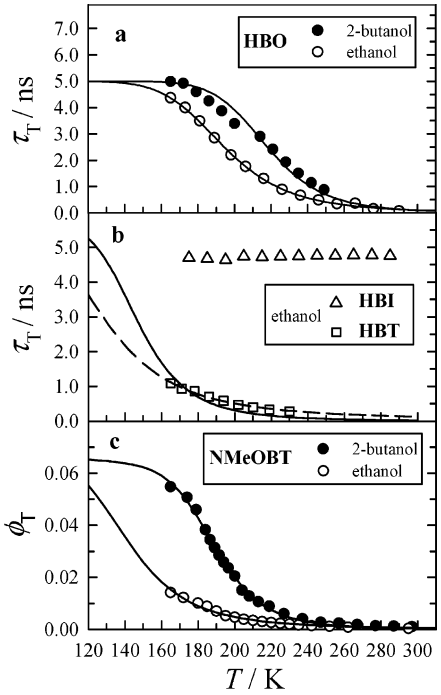

Figure 7. Temperature dependence of the fluorescence decay times τ_T of (a) HBO in ethanol and 2-butanol (obtained from the monoexponential fit of the fluorescence decay at 20 830 cm^{-1} (ethanol) and 20 000 cm^{-1} (2-butanol) with $\tilde{\nu}_{exc} = 30\,300\ cm^{-1}$), together with the fit of eq 1 to the experimental data; (b) HBT and HBI in ethanol (obtained from the monoexponential fit of the fluorescence decay at 19 610 cm^{-1} (HBT) and 22 220 cm^{-1} (HBI) with $\tilde{\nu}_{exc} = 31\,250\ cm^{-1}$), together with the fits of eq 1 to the experimental τ_T of HBT (see text); (c) Temperature dependence of the fluorescence quantum yield of NMeOBT in ethanol and 2-butanol (calculated from the fluorescence spectra of Figures 6b and 6c), together with the fit of eq 2 to the experimental data.

tions.[64,65] The fact that tautomer **T** is observed only in water, where the solubility of HPyBO is very low, hinders the use of other experimental techniques to determine the concentration relation [**T**]/[**N**].

Protonation of HPyBO in acid media ($pK_{a1} = 1.67$) could take place at the pyridine nitrogen or at the benzoxazole nitrogen. On the basis of the pK_a values of the protonated benzoxazole moiety ($pK_a = -0.13$)[66] and the protonated 3-hydroxypyridine moiety ($pK_a = 5.05$),[67] we assign the first protonation site of HPyBO to the pyridine nitrogen. Substitution of the benzoxazole O atom for the benzimidazole NH group causes a strong decrease in the basicity of the benzazole N(3) atom, as can be observed by the pK_a values of protonated benzimidazole ($pK_a = 5.53$)[66] and benzoxazole ($pK_a = -0.13$),[66] and those of protonated HBI ($pK_a = 5.48$)[12] and HBO (1.30).[14] This explains the different basicities of HPyBI ($pK_a = 5.00$, protonated at the benzimidazole nitrogen)[63] and HPyBO ($pK_a = 1.67$, protonated at the pyridine nitrogen). Additional evidence in favor of this assignment of the first protonation site of HPyBO comes from the fluorescence data in acid media that will be analyzed in the next section.

2. Interpretation of the Fluorescence Spectra and Lifetimes of HPyBO in Acetonitrile: Both the Neutral Form and the Monocation Undergo Phototautomerization. The dual fluorescence observed for HPyBO in acetonitrile (Figure 2b) indicates the presence of at least two fluorescent species in this solvent. Besides, as the excitation spectra monitored at both emission bands were different, the red- and blue-emission bands originate from two different ground-state species. An anomalous Stokes shift was observed between the red-emission band and its excitation spectrum, showing that the structure of the fluorescent species is different from that of the ground-state species and, therefore, that a transformation must take place in the excited state. Furthermore, this process must involve the hydroxyl group, because the fluorescence spectrum of the methoxy derivative (Figure 2a) did not show the red-emission band. Therefore, we propose that HPyBO undergoes a phototautomerization process involving an intramolecular proton transfer from the hydroxyl group to the benzoxazole nitrogen of the normal form **N*** to give tautomer **T*** (Scheme 1), similar to the related compounds HPyBI, HBI, HBO, and HBT.[4−6,60] For this process to occur, the normal form must be in a syn conformation, which allows the proton transfer through the intramolecular hydrogen bond between the hydroxyl group and the benzoxazole nitrogen. As the excitation spectrum of the red-shifted fluorescence band almost coincided with the absorption spectrum measured under the same conditions (Figure 2b), $\mathbf{N_{syn}}$ must be the major species present in the ground state.

SCHEME 1: Excitation and Deactivation Pathways of HPyBO in Acetonitrile

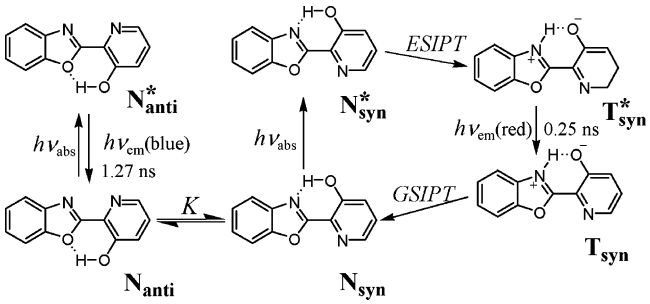

The weak blue-shifted emission band of HPyBO in acetonitrile (Figure 2b) overlapped its excitation spectrum, and, therefore, both spectra must be due to the same species. Since the emission spectrum was located at the same position as that of the methoxy derivative (Figure 2a), both compounds showed the same decay times (1.27 ns for HPyBO and 1.28 ns for OMePyBO), and their excitation spectra were very similar, it is clear that the minor ground-state component of HPyBO present in acetonitrile is a neutral form unable to tautomerize, that is, without the intramolecular hydrogen bond N···H−O. In this aprotic solvent, this neutral form is probably the closed $\mathbf{N_{anti}}$ rotamer of HPyBO, showing an intramolecular hydrogen bond between the hydroxyl group and the benzoxazole O (Chart 1). In protic solvents other "open" rotamers, with the N and OH groups hydrogen-bonded to the solvent, would probably exist.

The decay time of HPyBO **T*** form in acetonitrile (0.25 ns) was 15 times lower than that of the benzimidazole derivative HPyBI (3.7 ns).[60] Furthermore, it is observed in Table 2 that the fluorescence quantum yield of **T*** in acetonitrile was ∼37 times higher for HPyBI than that for HPyBO, and whereas for HPyBO, ϕ_T increased with the solvent viscosity, that of HPyBI was independent of viscosity. As the absorption and fluorescence spectra of both compounds are very similar, this suggests that the proton-transferred tautomer of the benzoxazole derivative experiences a viscosity-dependent radiationless deactivation pathway, absent for HPyBI. As previously noted, the same behavior was proved to hold for HBT.[32,37,38]

Turning to acid media, we showed in the previous section that the first protonation of HPyBO takes place at the pyridine nitrogen to give the monocation **C** (Scheme 2). Considering the similarity of the absorption and fluorescence excitation spectra of HPyBO and the methoxy derivative OMePyBO in

SCHEME 2: Excitation and Deactivation Pathways of HPyBO in Acidified Acetonitrile

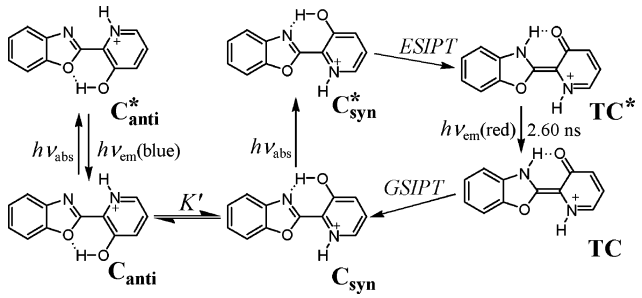

acid media (Figures 1 and 2), the last compound must also protonate at the pyridine nitrogen. Therefore, the fluorescence emission spectrum of OMePyBO in acidified methanol (Figure 2a) can be assigned to the emission of the cation protonated at the pyridine nitrogen. However, for HPyBO, dual fluorescence was observed in acidified acetonitrile (Figure 2c). The emission spectrum showed an intense structured band, red-shifted with respect to that of the monocation of the methoxy derivative, accompanied by a shoulder at ~24 000 cm^{-1}. Two different ground-state monocations must originate the dual fluorescence, as a different excitation spectrum was obtained at each emission band. The excitation spectrum monitored at the weak fluorescence band overlapped its emission spectrum and was very similar to that of the monocation of OMePyBO (Figures 2a and 2c), indicating that they are due to the monocation **C**. However, a big Stokes shift was observed between the maximum of the strong emission band and that of its excitation spectrum, this showing that the structure of the fluorescent species is different from that of the monocation being excited. Furthermore, the transformation taking place in the excited state must involve the OH group, as the monocation of the methoxy derivative OMePyBO, lacking the hydroxyl group, does not experience that process. We propose that **C*** experiences an ESIPT from the hydroxyl group to the benzoxazole nitrogen (similar to that observed for the neutral form **N***), to yield the tautomeric cation **TC*** (Scheme 2).

According to the previous assignment, the 2.6 ns decay time measured for HPyBO in acidified acetonitrile at $\tilde{\nu}_{em} < 22\,200$ cm^{-1} (i.e., at the strong emission band) must correspond to **TC***. Furthermore, process **C*** → **TC*** must be very rapid, as the fluorescence from **C*** was very weak, and showed a different excitation spectrum. This means that those **C** molecules yielding **TC*** upon excitation must be in a syn conformation, showing an intramolecular hydrogen bond between the OH group and the benzoxazole nitrogen already in the ground state (Scheme 2). This syn cation must be the main monocation present in the ground state, as the excitation spectrum of the red-emission band almost coincided with the absorption spectrum (Figure 2c). The minor ground-state component, responsible for the weak blue-shifted emission band and unable to yield **TC*,** is probably the anti rotamer $\mathbf{C_{anti}}$, with the phenyl ring rotated 180° with respect to the benzoxazole moiety, and exhibiting an intramolecular hydrogen bond between the benzoxazole O and the OH group (Scheme 2).

Finally, the protonated tautomer **TC*** showed, in acetonitrile, a decay time 10 times slower than that of **T*** (2.6 ns for **TC*** and 0.25 ns for **T***). Similarly, the fluorescence quantum yield in the same solvent under acidic conditions (ϕ_{acid}) (due to **TC*** and a minor amount of $\mathbf{C^*_{anti}}$) was also ~10 times higher than that of **T*** and showed no dependence with the solvent viscosity (Table 2). This seems to indicate that the viscosity-dependent radiationless decay experienced by **T*** is blocked upon protonation of **T*** at the pyridine nitrogen.

3. Interpretation of the Influence of Temperature and Viscosity on the Fluorescence of *o*-Hydroxyarylbenzazoles. The red-emission band, observed for HBO and HBT in ethanol, butanol (Figure 5), and other solvents, has been attributed to the $\mathbf{T^*_{syn}}$ tautomer resulting from ESIPT in $\mathbf{N^*_{syn}}$, whereas the blue-emission band has been reported to be due to light absorption by "closed" or "open" rotamers of $\mathbf{N_{syn}}$ (see $\mathbf{N_{anti}}$ in Chart 1) lacking the intramolecular hydrogen bond N····H−O that are, therefore, unable to undergo ESIPT.[5,10,23,24,37] However, the amount of these rotamers must be very small for HBO and HBT, because the excitation spectrum of the red-shifted fluorescence band matched the absorption spectrum in all the solvents studied. Therefore, the fluorescence quantum yields measured in the red-emission band of HBO and HBT (see Table 2) correspond to the $\mathbf{T^*_{syn}}$ tautomer.

The fluorescence quantum yield and lifetime of the **T*** tautomer are, in any solvent, much higher for HBI than for HBO and HBT, and they are also much higher for HPyBI than for its benzoxazole analog, HPyBO (Table 2, Figures 4 and 7). This confirms the existence of the long-recognized, efficient radiationless decay of the $\mathbf{T^*_{syn}}$ tautomers of the benzoxazole and benzothiazole compounds, which is absent for the benzimidazole derivatives. This radiationless process must be strongly dependent on the solvent viscosity, because the observed fluorescence quantum yield drastically increased with viscosity for the benzoxazole and benzothiazole compounds (Table 2). This confirms that the radiationless decay must involve a large-amplitude molecular motion that is inhibited in a highly viscous medium. In agreement with this, the tautomer fluorescence quantum yield increases with respect to that in solution when HBO is attached to DNA[22,23] or employed as the core of dendrimers,[19] as a result of the restricted-motion environment of both DNA and dendrimers.

NMeOBT, the analog of the HBT **T*** tautomer with a methyl group at the benzothiazole N3, shows an anti planar tautomer structure $\mathbf{T_{anti}}$ (Chart 1) in the ground state,[30] as confirmed by ^{1}H NMR.[67] The fluorescence spectrum of NMeOBT in alcohols (Figure 6a) showed only one band with a normal Stokes shift (located at approximately the same position as that of the HBT $\mathbf{T^*_{syn}}$), indicating that the fluorescent species is the same being excited, that is, $\mathbf{T^*_{anti}}$. This species also experiences a thermally activated radiationless decay, as evidenced by the data shown in Figures 6 and 7. Flash photolysis studies of NMeOBT showed also that this species undergoes a photoinduced anti-to-syn isomerization, followed by thermal recovery of the anti isomer.[31] The parallel behavior of $\mathbf{T^*_{syn}}$ and $\mathbf{T^*_{anti}}$ structures therefore suggests that a similar molecular motion takes place for both conformational isomers, and, therefore, that the syn → anti isomerization of HBO and HBT associated with the radiationless decay probably is not due to rotation of $\mathbf{T^*_{syn}}$ to reach a lower-energy $\mathbf{T^*_{anti}}$ structure.

Information about the temperature dependence of the tautomer radiationless decay can be obtained by analyzing the influence of temperature on the fluorescence lifetimes (τ_T) and the fluorescence quantum yields (ϕ_T). The fluorescence decay time of $\mathbf{T^*_{syn}}$ (or $\mathbf{T^*_{anti}}$ for NMeOBT) is given by

$$\tau_T = \frac{1}{k_T + k_{conf}}$$

where k_{conf} is the rate constant of the conformational change and k_T is the sum of all the radiative and nonradiative deactivation rate constants, except k_{conf}. If we assume that k_{conf}

TABLE 3: Parameters Obtained by Fitting eqs 1 and 2 to the Experimental Fluorescence Quantum Yields and Lifetimes of HPyBO, HBO, HBT, and NMeOBT in Various Solvents

	value			
parameter	HPyBO	HBO[b]	HBT	NMeOBT[b]
	solvent: acetone (E_η = 7.30 kJ/mol)[a]			
ϕ_T^0	0.205 ± 0.005			
A/k_T	(3 ± 1) × 10^4			
E_{obs}	19.1 ± 0.9 kJ/mol			
	solvent: ethanol (E_η = 13.25 kJ/mol)[a]			
τ_T^0	4.25 ns[c]	5.00 ± 0.10 ns	5.7 ns[d]	
ϕ_T^0				0.0554 ± 0.0013
A/k_T				(6 ± 3) × 10^3
E_{obs}	20.0 ± 1.0 kJ/mol	17.5 ± 1.1 kJ/mol	13.25 kJ/mol[e]	10.4 ± 0.6 kJ/mol
A	(2.8 ± 1.4) × 10^{12} s^{-1}	(1.0 ± 0.6) × 10^{13} s^{-1}	(8.9 ± 1.0) × 10^{12} s^{-1}	
	solvent: 2-butanol (E_η = 25.75 kJ/mol)[a]			
τ_T^0		5.00 ± 0.10 ns		
ϕ_T^0				0.0554 ± 0.0013
A/k_T				(1.7 ± 0.8) × 10^6
E_{obs}		25.75 kJ/mol		22.7 ± 0.8 kJ/mol
A		(3.0 ± 0.3) × 10^{14} s^{-1}		

[a] Calculated from the viscosities of ref 70. [b] A global fit of eq 1 to the experimental τ_T data in ethanol and 2-butanol was performed. [c] The experimental value of τ_T at low temperature was used. [d] The reported value in ethanol[37] was used. [e] The value of E_η in ethanol was used.

is the only temperature-dependent deactivation rate constant and that it shows an Arrhenius-type dependence on temperature ($k_{conf} = A \exp[-E_{obs}/(RT)]$), eqs 1 and 2 are easily derived, where τ_T^0 and ϕ_T^0 are, respectively, the fluorescence lifetime and quantum yield of the tautomer in the absence of any conformational change.

$$\tau_T = \frac{\tau_T^0}{1 + (A/k_T)\exp[-E_{obs}/(RT)]} \quad (1)$$

$$\phi_T = \frac{\phi_T^0}{1 + (A/k_T)\exp[-E_{obs}/(RT)]} \quad (2)$$

Note that, for HPyBO, HBO, and HBT in alcohols, the intensity of the emission band of $\mathbf{T^*_{syn}}$ changed with temperature not only because of the temperature dependence of ϕ_T, but also because the ground-state equilibrium between $\mathbf{N_{syn}}$ and $\mathbf{N_{anti}}$ is also a function of temperature ($\mathbf{N_{anti}}$ is favored at lower temperatures, as can be deduced from the increasing intensity of the blue-emission band upon lowering the temperature; see Figures 3a and 5). This fact determines that a different (and unknown) amount of each conformer is excited when temperature is changed. Therefore, for these compounds in alcohols, the change of ϕ_T with temperature could not be measured, and only the influence of temperature on the fluorescence decay time of $\mathbf{T^*_{syn}}$ was determined. For HPyBO in acetone, only fluorescence from $\mathbf{T^*_{syn}}$ was observed in all the temperature range studied (Figure 3b), and, therefore, the change of ϕ_T with temperature could be measured. The parameters obtained from the fit of eq 1 or eq 2 to the experimental τ_T and ϕ_T data of all the compounds studied in various solvents are collected in Table 3.

The observed activation energy (E_{obs}) can be approximated by eq 3,[68,69]

$$E_{obs} = E_a + \alpha E_\eta \quad (3)$$

where E_a is the intrinsic activation energy of the conformational change, E_η represents the activation energy for the solvent viscous flow, and $0 < \alpha \leq 1$.

For HPyBO, the fits of eq 1 to τ_T (ethanol) and of eq 2 to ϕ_T (acetone) are shown in Figures 4a and 4b, respectively. The quality of the fit was good and, as observed in Table 3, for both solvents, E_{obs} was ~20 kJ/mol, this value being higher than the activation energy of viscous flow of both acetone (7.30 kJ/mol) and ethanol (13.25 kJ/mol).[70] This suggests that, for HPyBO, the conformational change experienced by $\mathbf{T^*_{syn}}$ shows an intrinsic activation barrier, as a barrierless process would lead (eq 3) to $E_{obs} \approx E_\eta$. For HBO, a global fit of eq 1 to the experimental τ_T in both ethanol and 2-butanol (Figure 7a and Table 3) was performed under the assumption that τ_T^0 has the same value in both alcohols. The analysis led to a value of τ_T^0 = 5.00 ns, similar to that reported for Mordziński et al.[15] for this compound (5.6 ns) in 3-methylpentane (3-MP). Furthermore, the fit in ethanol (Table 3) provided a value of E_{obs} = 17.5 kJ/mol, this value being slightly higher than the E_η of ethanol, whereas in 2-butanol, a good fit was obtained with $E_{obs} = E_\eta$ (25.75 kJ/mol). On the other hand, Mordziński et al.[15] obtained a value of E_{obs} = 15 kJ/mol in 3-MP; this figure is also higher than the E_η of 3-MP (6.85 kJ/mol).[70] These findings seem to indicate that, in solvents of low viscosity, the conformational change of $\mathbf{T^*_{syn}}$ shows a small activation energy for HBO, which becomes insignificant compared to the E_η in solvents of high viscosity.

The analysis of the fluorescence decay times of HBT in ethanol is complicated by the fact that the shape of the $\tau_T - T$ curve (Figure 7b) is not known in the low-temperature region. The data were analyzed by fixing τ_T^0 with the same value as that reported by Brown et al.[37] for this compound in ethanol (5.7 ns). The fit (the dashed line in Figure 7b) led to a value of E_{obs} = 7.2 ± 0.3 kJ/mol, clearly lower than the E_η of ethanol, and to a pre-exponential factor ((1.4 ± 0.3) × 10^{11} s^{-1}) about one order of magnitude lower than those obtained for the other hydroxyarylbenzazoles (Table 3). The data were also analyzed by fixing τ_T^0 and $E_{obs} = E_\eta$ (the solid line in Figure 7b and Table 3). This analysis provides a value of A = (8.9 ± 1.0) × 10^{12} s^{-1}, very similar to those of the other compounds studied here, but the quality of the fit slightly decreases. Despite the uncertainty in E_{obs}, it seems clear from the data analysis that, for HBT in ethanol, $E_{obs} \leq E_\eta$, which suggests a barrierless conformational change for the tautomer in this solvent. Al-Soufi

et al.[33] reported, for HBT in 3-MP, a value of $E_{obs} = 16.2$ kJ/mol, higher than the value of E_η for 3-MP (6.85 kJ/mol);[70] this points to a process with an activation barrier in this solvent.

A global analysis of the $\phi_T - T$ data in ethanol and 2-butanol was carried out for NMeOBT, considering that ϕ_T^0 has the same value in both alcohols. The fit (Figure 7c and Table 3) led to, in both ethanol and 2-butanol, an observed activation energy slightly lower than the corresponding E_η, and, therefore, a barrierless conformational change of $\mathbf{T^*_{anti}}$ must be operating for this compound in alcohols.

Pre-exponential factors A (Table 3) on the order of $10^{12}-10^{13}$ s^{-1} were obtained for these compounds in ethanol, these values being on the same order as those reported for HBO[15] and HBT[33] in 3-MP (9×10^{11} s^{-1} and 8×10^{12} s^{-1}, respectively). Moreover, when changing the solvent from ethanol to 2-butanol, A increased by a factor of ~30 for HBO and by a factor of ~280 for NMeOBT. A rise in the phototoisomerization pre-exponential factor upon increasing the solvent E_η was also reported, for example, for a cyanine dye in *n*-alcohols[71] and for various stilbenes when changing the solvent from alkanes to glycerol.[72−74]

Finally, the observed trend in E_{obs} for the different compounds studied here in a given solvent will be discussed in the next section.

4. Role of Charge Transfer on the Radiationless Decay of *o*-Hydroxyarylbenzazoles Tautomer. Potter et al.[37] advanced the hypothesis that the thermally activated radiationless decay of the HBT proton-transferred tautomer is caused by a charge-transfer process and is associated with large-angle torsional motion. High-level quantum mechanical calculations on related ESIPT molecules of the hydroxyphenyltriazole type also predict a charge transfer of almost a full electron from the phenol portion to the triazole portion, associated with large-amplitude conformational motion of the proton-transferred tautomer.[47,48] Similar results were obtained in other ESIPT molecules.[43−45] To further test this hypothesis experimentally, we studied the relationship between the effectiveness of the radiationless deactivation and the intramolecular redox properties of different model compounds.

In the series HBI, HBO, HBT, and NMeOBT (Chart 1), the tautomeric structures share the electron donor (a phenolate moiety), differing only in the electron acceptor (a benzazole ring protonated or methylated at the N3). We investigated the redox properties of the protonated benzazole rings through the model 3-methylbenzazolium methyl sulfates NMeBI, NMeBO, and NMeBT (Chart 1). The model compound for HBI should be, in fact, the analog of NMeBI with a H atom instead of a methyl group at the N1 site. We could not use this compound, but we must keep in mind that NMeBI, because of the extra methyl group, is a better electron acceptor than the protonated benzimidazolium moiety of the HBI tautomer. The cyclic voltammetry measurements of these model compounds in acetonitrile led to reduction peaks of approximately −2.1, −1.6, and −1.4 V for NMeBI, NMeBO, and NMeBT, respectively, indicating that NMeBT is the best oxidant of the series, closely followed by NMeBO, whereas NMeBI is the worst oxidant of the group. In agreement with this, in dimethyl sulfoxide, the ^{1}H NMR chemical shift of the proton attached to the C2 atom of the benzazolium salts (position where the phenolic ring is attached to the benzazole moiety in the tautomeric structures) was 9.6 ppm for NMeBI, 10.6 ppm for NMeBO, and 10.5 ppm for NMeBT. These results show also that the oxidizing character of the benzoxazolium and benzothiazolium salts is higher than that of the benzimidazolium derivative. Therefore, the electron acceptor strength in the ground state increases from the benzimidazolium to the benzoxazolium and benzothiazolium cations (see Chart 2). To evaluate the charge-accepting ability of the three excited protonated benzazole moieties, the electronic excitation energy of each compound must be taken into account. As estimation of this magnitude, the fluorescence emission maxima of the tautomers will be used, because the absorption spectra of the tautomers are not known for all compounds of the series. The emission maxima of the tautomers decrease from HBI to HBO and HBT (at 22 000, 20 000, and 18 500 cm^{-1}, respectively). Using the Rehm−Weller equation[75] to make a rough estimation, these results point to the fact that the feasibility of the intramolecular charge-transfer process in the excited-state should be much lower for the $\mathbf{T^*_{syn}}$ form of HBI than for HBO and HBT, as the higher excitation energy of HBI does not compensate for the poor charge-accepting character of the benzimidazolium moiety in the ground state.

CHART 2: Relative Strength of the Electron Donors and the Electron Acceptors in the Tautomers of the *o*-Hydroxyarylbenzazoles

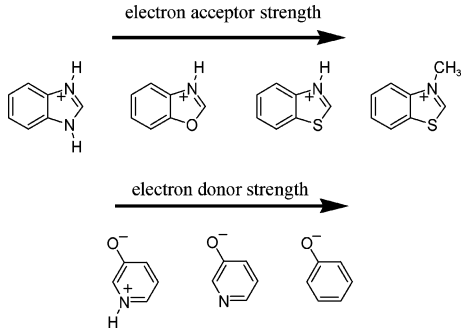

In summary, our results indicate that the efficiency of the hypothetical CT from the phenolate group to the protonated benzazole moiety for the tautomers of the *o*-hydroxyphenylbenzazoles would increase in the following order: HBI ≪ HBO < HBT < NMeOBT (the methyl group at the benzothiazole nitrogen makes NMeOBT a stronger electron acceptor than the parent HBT). This prediction is in good agreement with the experimental finding (Table 2) that the fluorescence quantum yield of the tautomer decreases (and, therefore, the radiationless decay is more efficient) in the series ϕ_T(HBI) ≫ ϕ_T(HBO) > ϕ_T(HBT) > ϕ_T(NMeOBT), the highest value being observed for HBI, for which no viscosity-dependent radiationless decay was detected. Furthermore, the values in Table 2 show that ϕ_T is 20−40 times higher for HPyBI than for HPyBO, in accordance with the fact that their $\mathbf{T^*_{syn}}$ structures share the same electron donor (a deprotonated pyridinol ring), but HPyBO exhibits a better electron acceptor (benzoxazolium) than HPyBI (benzimidazolium).

In agreement with the CT hypothesis, a correlation between the observed fluorescence quantum yield and the strength of the electron donor group is also observed for the tautomers of HBO and HPyBO and the tautomeric cation of HPyBO, all of them sharing benzoxazolium as electron acceptor. It is observed in Table 2 that, in any solvent, ϕ_{acid}(HPyBO) > ϕ_T(HPyBO) > ϕ_T(HBO), and, under the CT hypothesis, this means that the strength of the electron donor group (Chart 2) must increase in the following order: **TC***(HPyBO) < $\mathbf{T^*_{syn}}$(HPyBO) < $\mathbf{T^*_{syn}}$(HBO). This should be indeed the case, because substitution of the N atom (more electronegative than C) for a C3′ atom at the phenolate ring in the tautomer of HBO to yield the pyridine ring of HPyBO weakens its electron donor strength.

SCHEME 3: Mechanism Proposed for the Coupled Intramolecular Proton and Charge Transfer in the First Excited Singlet State of HBO, HBT, and HPyBO: (1) Excited-State Intramolecular Proton Transfer and (2) Charge Transfer and Large-Amplitude Conformational Change[a]

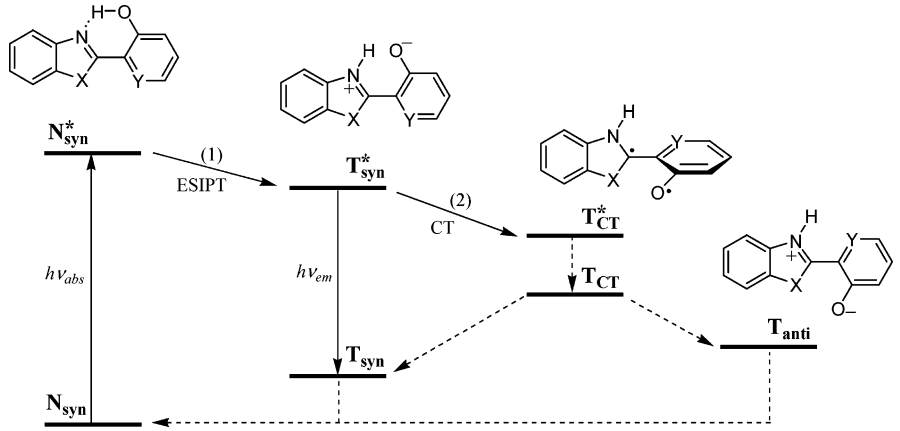

[a] The real structure of the charge-transfer species $\mathbf{T}^*_{\mathbf{CT}}$ is unknown. The dashed arrows outline the back charge transfer, planarization and back proton transfer, not studied in this work. See text for references to studies on the microsecond dynamics of HBO and HBT, which include detection of $\mathbf{T}_{\mathbf{anti}}$, its mechanism of taumerization in the ground state, and intersystem crossing from $\mathbf{T}^*_{\mathbf{syn}}$. These steps have not been included here to simplify the scheme.

If the pyridine nitrogen is then protonated (as in **TC*** of HPyBO), the electron donor strength dramatically decreases, as the NH^+ site attracts the ring negative charge. In fact, for **TC***, no CT or conformational change should take place, as no dependence of the fluorescence quantum yield with solvent viscosity or temperature was observed.

All these results validate the hypothesis that, for the HPyBO, HBO, and HBT $\mathbf{T}^*_{\mathbf{syn}}$ tautomer, and for the NMeOBT $\mathbf{T}^*_{\mathbf{anti}}$ form, the radiationless decay observed involves an intramolecular CT from the dissociated phenol or pyridinol moiety (donor) to the protonated or methylated benzazole (acceptor). The previous proton transfer in HPyBO, HBO, and HBT is the requirement for CT to occur, as the proton transfer generates the molecular structure with the appropriate intramolecular redox properties. When this structure is formed, an electron displacement toward the benzazolium moiety takes place, coupled with a large-amplitude conformational change, giving the charge-transferred species $\mathbf{T}^*_{\mathbf{CT}}$(Scheme 3).

The structure of $\mathbf{T}^*_{\mathbf{CT}}$ shown in Scheme 3 is only indicative, as the real structure is unknown. Quantum mechanical ab initio calculations on the related azoles 2-(2′-hydroxyphenyl)oxazole and 2-(2′-hydroxyphenyl)-4-methylthiazole predict that the excited proton-transferred tautomer has a small energy barrier for rotation, and an energy minimum was found for a twisted and bent conformation.[45] The twisted structure possesses a biradicaloid nature and shows an increased electron density in the oxazole or thiazole ring that leads to rehybridization and pyramidalization of the five-membered ring subsystem. High-level theoretical studies on the related family of 2-(2′-hydroxyphenyl)benzotriazole UV photostabilizers showed a folded structure of the proton-transferred form with concomitant CT from the phenol ring to the triazole ring as relevant in the mechanism of the fast radiationless decay.[47,48]

The fluorescence of the charge-transferred species $\mathbf{T}^*_{\mathbf{CT}}$ was not detected in this work, probably because of a very small energy gap , $S_1 - S_0$ (or even a conical intersection), and, consequently, very fast radiationless decay of this species, as was found in quantum mechanical calculations on related structures.[44,45,47−49] Thus, it can be stated that substituents in the ESIPT molecule that favor the CT from the proton donor to the proton acceptor moiety will increase the nonradiative decay and, consequently, decrease the fluorescence quantum yield. This has been proven to be true for hydroxyphenylbenzotriazole UV photostabilizers, which showed increased photostability when the benzotriazole ring incorporates electron-withdrawing groups.[54] Moreover, when the electron-withdrawing substituents were introduced in the proton donor moieties of several ESIPT molecules, their fluorescence quantum yield significantly increased.[55]

After deactivation to the ground state, the twisted or folded tautomer $\mathbf{T}_{\mathbf{CT}}$ would undergo a conformational relaxation toward the two planar forms, $\mathbf{T}_{\mathbf{syn}}$ and $\mathbf{T}_{\mathbf{anti}}$ (see Scheme 3). $\mathbf{T}_{\mathbf{syn}}$ would revert rapidly to $\mathbf{N}_{\mathbf{syn}}$ by ground-state intramolecular proton transfer, but the difficulty of the back-proton transfer for $\mathbf{T}_{\mathbf{anti}}$ in the absence of protic substances makes the process slower, allowing the detection of $\mathbf{T}_{\mathbf{anti}}$ as a long-lived transient species in flash photolysis experiments of HBO and HBT.[16,30−34] This mechanism is in accordance with the detailed temperature-dependent studies on HBT solutions carried out by Al-Soufi et al., who found different temperature dependencies of the quantum yields of fluorescence and syn−anti isomerization.[33]

The microsecond dynamics of the back-proton transfer of HBO and HBT $\mathbf{T}_{\mathbf{anti}}$ tautomer, together with the intersystem crossing and tautomerization in the triplet state, have been studied by several authors by transient absorption, two-step laser excitation, and phosophorescence techniques.[4−6,15−18,29−36] Because of the ultrafast ESIPT of the excited normal form $\mathbf{N}^*_{\mathbf{syn}}$, intersystem crossing can only occur from the proton-transferred tautomer $\mathbf{T}^*_{\mathbf{syn}}$, yielding the triplet tautomer, from which the triplet normal form may arise. The relative triplet energies of the normal and tautomer forms depend on the nature of the derivative being studied (almost equal for HBO, slightly lower for the triplet normal form in deuterated HBO, and lower for the triplet tautomer in HBT).[17,18,31,35,36] The back-proton transfer of the ground-state HBO and HBT anti tautomer is catalyzed by traces of protic compounds, and in dry nonpolar solvents, it decays in a second-order reaction by mutual hydrogen exchange: $2\mathbf{T}_{\mathbf{anti}} \rightarrow 2\mathbf{N}_{\mathbf{anti}} \rightarrow 2\mathbf{N}_{\mathbf{syn}}$.[16,33] A similar mechanism has been presented for related structures.[53,76] To simplify Scheme 3, we have not included the intersystem crossing from $\mathbf{T}^*_{\mathbf{syn}}$ and the mechanism of ground-state tautomerization, not studied in this work.

Finally, the observed activation energies of the radiationless decay, analyzed in the previous section, can also be interpreted

under the assumption of a CT process. It is known that the activation energy for a CT process usually decreases as the exergonicity of the CT increases.[75] We have already shown that the efficiency of the CT process of the excited tautomer increases in the order HPyBO < HBO < HBT < NMeOBT, and, accordingly, we would expect a decrease in the activation energy, for a given solvent, upon going from HPyBO to NMeOBT in that series. The fact that, in ethanol (Table 3), the radiationless decay showed an intrinsic activation energy ($E_{obs} > E_\eta$) for HPyBO and HBO, whereas for HBT and NMeOBT, the process is barrierless ($E_{obs} \leq E_\eta$), further supports our proposal that, for these compounds, the radiationless decay and concomitant large-amplitude motion of the excited tautomer is associated with CT from the deprotonated phenol or pyridinol ring to the protonated benzazole moiety.

Conclusions

The excited-state behavior of the *o*-hydroxyarylbenzazoles 2-(2′-hydroxyphenyl)benzoxazole (HBO), 2-(2′-hydroxyphenyl)-benzothiazole (HBT), 2-(2′-hydroxyphenyl)benzimidazole (HBI), 2-(3′-hydroxy-2′-pyridyl)benzimidazole (HPyBI), and 2-(3′-hydroxy-2′-pyridyl)benzoxazole (HPyBO), and the related compound 2-(3-methyl-1,3-benzothiazol-3-ium-2-yl)benzenolate (NMeOBT), have been investigated by means of steady-state and time-resolved fluorescence. The fluorescence quantum yield and lifetime of the tautomer generated after ESIPT have been found to be strongly dependent on temperature and solvent viscosity for all compounds except HBI and HPyBI.

The new *o*-hydroxyarylbenzazole HPyBO exists in the ground state mainly as the normal hydrogen-bonded form $\mathbf{N_{syn}}$ in aprotic solvents and in neutral aqueous solution, although small amounts of the $\mathbf{N_{anti}}$ conformer and the $\mathbf{T_{syn}}$ tautomer (this one only in water) have been detected. After excitation, $\mathbf{N^*_{syn}}$ undergoes an ultrafast ESIPT from the hydroxyl group to the benzoxazole N3 to give the $\mathbf{T^*_{syn}}$ tautomer. Protonation of HPyBO takes place at the pyridine nitrogen, giving the cation **C**. For this compound, small quantities of the $\mathbf{C_{anti}}$ conformer have been detected in acidified acetonitrile; however, the main ground-state conformer is the hydrogen-bonded monocation $\mathbf{C_{syn}}$, which, in the excited state, experiences fast excited-state intramolecular proton transfer (ESIPT) from the OH group to the benzoxazole nitrogen to yield the tautomeric cation $\mathbf{TC}^*$.

The excited tautomers $\mathbf{T^*_{syn}}$ of HPyBO, HBO, and HBT (as well as $\mathbf{T^*_{anti}}$ of NMeOBT) experience a temperature- and viscosity-dependent radiationless transition associated with a large-amplitude conformational change, which does not occur for the structurally related benzimidazole derivatives HBI and HPyBI. In ethanol, this conformational change shows an intrinsic activation energy for HPyBO and HBO; however, it is barrierless for HBT and NMeOBT and controlled instead by the solvent dynamics.

It has been shown that the conformational change of the tautomer is most likely to be connected with a charge migration from the dissociated phenol or pyridinol ring (donor) to the protonated benzazole (acceptor), leading to a charge-transfer species, $\mathbf{T^*_{CT}}$, whose emission was not detected. After deactivation of $\mathbf{T^*_{CT}}$ to the ground state, conformational relaxation would yield the planar tautomers $\mathbf{T_{syn}}$ and $\mathbf{T_{anti}}$, which, after proton transfer, regenerate the more-stable ground-state tautomer $\mathbf{N_{syn}}$. Essential for the charge transfer and conformational changes of these *o*-hydroxyarylbenzazoles is the previous intramolecular proton-transfer step, which creates the excited-state structure with the suitable electron-donor/electron-acceptor pair. Therefore, the process described may be considered to be an example of a proton-coupled charge transfer.

Acknowledgment. We thank the Spanish Ministry of Science and Technology and the European Union−ERDF (Project No. CTQ2004-07683-C02-01/BQU), and the Xunta de Galicia (DXID, Project No. PGIDIT05PXIC20905PN and Infraestructura Program) for financial support of this work.

References and Notes

(1) Müller, A., Ratajczak, H., Junge, W., Diemann, E., Eds. *Electron and Proton Transfer in Chemistry and Biology*; Elsevier: Amsterdam, 1992.
(2) Malmström, Bo G. In *Electron Transfer in Chemistry*, Balzani, V., Ed.; Wiley−VCH: Weinheim, Germany, 2001; Vol. 3, pp 39−52.
(3) Faxén, K.; Gilderson, G.; Ädelroth, P.; Brzezinski, P. *Nature* **2005**, *437*, 286.
(4) Formosinho, S. J.; Arnaut, L. G. *J. Photochem. Photobiol. A* **1993**, *75*, 21.
(5) Ormson, S. M.; Brown, R. G. *Prog. React. Kinet.* **1994**, *19*, 45.
(6) Waluk, J. In *Conformational Analysis of Molecules in Excited States*; Waluk, J., Ed.; Wiley−VCH: New York, 2000; Chapter 2.
(7) Williams, D. L.; Heller, A. *J. Phys. Chem.* **1970**, *74*, 4473.
(8) Ríos, M. A.; Ríos, M. C. *J. Phys. Chem.* **1998**, *102*, 1560.
(9) Sinha, H. K.; Dogra, S. K. *Chem. Phys.* **1986**, *102*, 337.
(10) (a) Das, K.; Sarkar, N.; Majumdar, D.; Bhattacharyya, K. *Chem. Phys. Lett.* **1992**, *198*, 443. (b) Das, K.; Sarkar, N.; Ghosh, A. K.; Majumdar, D.; Nath, D. N.; Bhattacharyya, K. *J. Phys. Chem.* **1994**, *98*, 9126.
(11) Douhal, A.; Amat-Guerri, F.; Lillo, M. P.; Acuña, A. U. *J. Photochem. Photobiol. A* **1994**, *78*, 127.
(12) Mosquera, M.; Penedo, J. C.; Ríos Rodríguez, M. C.; Rodríguez-Prieto, F. *J. Phys. Chem.* **1996**, *100*, 5398.
(13) Cohen, M. D.; Flavian, S. *J. Chem. Soc. B* **1967**, 317.
(14) Mordziński, A.; Grabowska, A. *Chem. Phys. Lett.* **1982**, *90*, 122.
(15) Mordziński, A.; Grellmann, K. H. *J. Phys. Chem.* **1986**, *90*, 5503.
(16) Stephan, J. S.; Grellmann, K. H. *J. Phys. Chem.* **1995**, *99*, 10066.
(17) (a) Al-Soufi, W.; Grellmann, K. H.; Nickel, B. *J. Phys. Chem.* **1991**, *95*, 10503. (b) Eisenberger, H.; Nickel, B.; Ruth, A. A.; Al-Soufi, W.; Grellmann, K. H.; Novo, M. *J. Phys. Chem.* **1991**, *95*, 10509.
(18) (a) Rodríguez-Prieto, M. F.; Nickel, B.; Grellmann, K. H.; Mordziński, A. *Chem. Phys. Lett.* **1988**, *146*, 387. (b) Nickel, B.; Rodríguez-Prieto, M. F. *Chem. Phys. Lett.* **1988**, *146*, 393.
(19) Ohshima, A.; Momotake, A.; Nagahata, R.; Arai, T. *J. Phys. Chem. A* **2005**, *109*, 9731.
(20) Ogawa, A. K.; Abou-Zied, O. K.; Tsui, V.; Jimenez, R.; Case, D. A.; Romesberg, F. E. *J. Am. Chem. Soc.* **2000**, *122*, 9917.
(21) Dupradeau, F. Y.; Case, D. A.; Yu, C.; Jimenez, R.; Romesberg, F. E. *J. Am. Chem. Soc.* **2005**, *127*, 15612.
(22) Abou-Zied, O. K.; Jimenez, R.; Romesberg, F. E. *J. Am. Chem. Soc.* **2001**, *123*, 4613.
(23) Wang, H.; Zhang, H.; Abou-Zied, O. K.; Yu, C.; Romesberg, F. E.; Glasbeek, M. *Chem. Phys. Lett.* **2003**, *367*, 599.
(24) Abou-Zied, O. K.; Jimenez, R.; Thompson, E. H. Z.; Millar, D. P.; Romesberg, F. E. *J. Phys. Chem. A* **2002**, *106*, 3665.
(25) Arten-Engeland, Th.; Bultmann, T.; Ernsting, N. P.; Rodríguez, M. A.; Thiel, W. *Chem. Phys.* **1992**, *163*, 43.
(26) Ríos, M. A.; Ríos, M. C. *J. Phys. Chem.* **1995**, *99*, 12456.
(27) Fernández-Ramos, A.; Rodríguez-Otero, J.; Ríos, M. A.; Soto, J. *J. Mol. Struct. Theochem.* **1999**, *489*, 255.
(28) Lochbrunner, S.; Stock, K.; Riedle, E. *J. Mol. Struct.* **2004**, *700*, 13.
(29) Itoh, M.; Fujiwara, Y. *J. Am. Chem. Soc.* **1985**, *107*, 1561.
(30) Nagaoka, S.; Itoh, A.; Mukai, K.; Nagashima, U. J. *Phys. Chem.* **1993**, *97*, 11385.
(31) Ikegami, M.; Arai, T. *J. Chem. Soc. Perkin Trans.* **2002**, *2*, 1296.
(32) Brewer, W. E.; Martinez, M. L.; Chou, P. T. *J. Phys. Chem.* **1990**, *94*, 1915.
(33) Al-Soufi, W.; Grellmann, K. H.; Nickel, B. *Chem. Phys. Lett.* **1990**, *174*, 609.
(34) Becker, R. S.; Lenoble, C.; Zein, A. *J. Phys. Chem.* **1987**, *91*, 3509.
(35) Chou, P.-T.; Studer, S. L.; Martinez, M. L. *Chem. Phys. Lett.* **1991**, *178*, 393.
(36) Chou, P.-T.; Martinez, M. L.; Studer, S. L. *Chem. Phys. Lett.* **1992**, *195*, 586.
(37) Potter, C. A.; Brown, R. G.; Vollmer, F.; Rettig, W. *J. Chem. Soc. Faraday Trans.* **1994**, *90*, 59.
(38) Barbara, P. F.; Brus, L. E.; Rentzepis, P. M. *J. Am. Chem. Soc.* **1980**, *102*, 5631.
(39) (a) Elsaesser, T.; Schmetzer, B.; Lipp, M.; Bäuerle, R. J. *Chem. Phys. Lett.* **1988**, *148*, 112. (b) Laermer, F.; Elsaesser, T.; Kaiser, W. *Chem. Phys. Lett.* **1988**, *148*, 119.
(40) Frey, W.; Laermer, F.; Elsaesser, T. *J. Phys. Chem.* **1991**, *95*, 10391.
(41) (a) Lochbrunner, S.; Wurzer, A. J.; Riedle, E. *J. Phys. Chem. A* **2003**, *107*, 10580. (b) Vivie-Riedle, R.; De Waele, V.; Kurtz, L.; Riedle, E. *J. Phys. Chem. A* **2003**, *107*, 10591.

(42) Rini, M.; Kummrov, A.; Dreyer, J.; Nibbering, E. T. J.; Elsaesser, T. *Faraday Discuss.* **2003**, *122*, 27.

(43) Vollmer, F.; Rettig, W. *J. Photochem. Photobiol. A* **1996**, *95*, 143.

(44) LeGourriérec, D.; Kharlanov, V.; Brown, R. G.; Rettig, W. *J. Photochem. Photobiol. A* **1998**, *117*, 209.

(45) LeGourriérec, D.; Kharlanov, V.; Brown, R. G.; Rettig, W. *J. Photochem. Photobiol. A* **2000**, *130*, 101.

(46) Kramer, H. E. A. In *Photochromism. Molecules and Systems*; Dürr, H., Bouas-Laurent, H., Eds.; Elsevier: Amsterdam, 1990; pp 654−684.

(47) Estevez, C. A.; Bach, R. D.; Has, K. C.; Schneider, W. F. *J. Am. Chem. Soc.* **1997**, *119*, 5445.

(48) Paterson, M. J.; Robb, M. A.; Blancafort, L.; DeBellis, A. D. *J. Am. Chem. Soc.* **2004**, *126*, 2912.

(49) Paterson, M. J.; Robb, M. A.; Blancafort, L.; DeBellis, A. D. *J. Phys. Chem. A* **2005**, *109*, 7527.

(50) Goeller, G.; Rieker, J.; Maier, A.; Stezowski, J. J.; Daltrozzo, E.; Neureiter, M.; Port, H.; Wiechmann, M.; Kramer, H. E. A. *J. Phys. Chem.* **1988**, *92*, 1452.

(51) Stueber, G. J.; Kieninger, M.; Schettler, H.; Busch, W.; Goeller, B.; Franke, J.; Kramer, H. E. A.; Hoier, H.; Henkel, S.; Fischer, P.; Port.; H.; Hirsch, T.; Rytz, G.; Birbaum, J.-L. *J. Phys. Chem.* **1995**, *99*, 10097.

(52) Keck, J.; Stüber, G. J.; Kramer, H. E. A. *Angew. Makromol. Chem.* **2003**, *252*, 119.

(53) Moriyama, M.; Kawakami, Y.; Tobita, S.; Shizuka, H. *Chem. Phys.* **1998**, *231*, 205.

(54) Suhadolnik, J. C.; DeBellis, A. D.; Hendricks-Guy, C.; Iyengar, R.; Wood, M. G. *J. Coat. Technol.* **2002**, *74*, 55.

(55) Doroshenko, A. O.; Posokhov, E. A.; Verezubova, A. A.; Ptyagina, L. M.; Skripkina, V. T.; Shershukov, V. M. *Photochem. Photobiol. Sci.* **2002**, *1*, 92.

(56) Xiao, D.; Zhang, G.; Wang, H.; Tang, G.; Chen, W. *J. Nonlinear Opt. Phys. Mater.* **2000**, *9*, 309.

(57) Hillebrand, S.; Segala, M.; Buckup, T.; Correia, R. R. B.; Horowitz, F.; Stefani, V. *Chem. Phys.* **2001**, *273*, 1.

(58) Chang, S. M.; Hsueh, K. L.; Huang, B. K.; Wu, J. H.; Liao, C. C.; Lin, K. C. *Surf. Coat. Technol.* **2006**, *200*, 3278.

(59) Chou, P. T. *J. Chin. Chem. Soc.* **2001**, *48*, 651.

(60) Rodríguez-Prieto, F.; Ríos Rodríguez, M. C.; Mosquera González, M.; Ríos Fernández, M. A. *J. Phys. Chem.* **1994**, *98*, 8666.

(61) Melhuish, W. H. *J. Phys. Chem.* **1961**, *65*, 229.

(62) Demas, J. N.; Crosby, G. A. *J. Phys. Chem.* **1971**, *75*, 991.

(63) Mosquera, M.; Ríos Rodríguez, M. C.; Rodríguez-Prieto, F. *J. Phys. Chem. A* **1997**, *101*, 2766.

(64) Bräuer, M.; Mosquera, M.; Pérez-Lustres, J. L.; Rodríguez-Prieto, F. *J. Phys. Chem. A* **1998**, *102*, 10736.

(65) Pérez-Lustres, J. L.; Bräuer, M.; Mosquera, M.; Clark, T. *Phys. Chem. Chem. Phys.* **2001**, *3*, 3569.

(66) Katritzky, A. R. *Handbook of Heterocyclic Chemistry*; Pergamon Press: New York, 1985.

(67) Foces-Foces, C.; Llamas-Saiz, A. L.; Claramunt, R. M.; Cabildo, P.; Elguero, J. *J. Mol. Struct.* **1998**, *440*, 193.

(68) Rettig, W.; Fritz, R.; Braun, D. *J. Phys. Chem. A* **1997**, *101*, 6830.

(69) Grabowski, Z. R.; Rotkiewicz, K.; Rettig, W. *Chem. Rev.* **2003**, *103*, 3899.

(70) Lax, E., Ed. *Taschenbuch Für Chemiker und Physiker. Makroskopische Physikalisch-Chemische Eigenschaffen*; Springer−Verlag: Berlin, 1967.

(71) Korppi-Tommola, J. E. I.; Hakkarainen, A.; Hukkla, T.; Subbi, J. *J. Phys. Chem.* **1991**, *95*, 8482.

(72) Saltiel, J.; D'Agostino, J. T. *J. Am. Chem. Soc.* **1972**, *94*, 6445.

(73) Saltiel, J.; Sun, Y.-P. *J. Phys. Chem.* **1989**, *93*, 6246.

(74) Wiemmers, K. L.; Kauffman, J. F. *J. Phys. Chem. A* **2001**, *105*, 823.

(75) Kavarnos, G. J. *Fundamentals of Photoinduced Electron Transfer*; VCH: New York, 1993.

(76) Stephan, J. S.; Ríos Rodríguez, C.; Grellmann, K. H.; Zachariasse, K. A. *Chem. Phys.* **1994**, *186*, 435.

(77) Murov, S. L., Carmichael, I., Hug, G. L., Eds. *Handbook of Photochemistry*; Marcel Dekker: New York, 1993.